AIAA 2000-0755

Numerical Study of Wake Vortex Behavior in Turbulent Domains with Ambient Stratification

George F. Switzer
Research Triangle Institute
Hampton, VA

Fred H. Proctor
NASA Langley Research Center
Hampton, VA

38th Aerospace Sciences Meeting & Exhibit
January 10-13, 2000 / Reno, NV

AIAA-2000-0755

NUMERICAL STUDY OF WAKE VORTEX BEHAVIOR IN TURBULENT DOMAINS WITH AMBIENT STRATIFICATION

George F. Switzer*
Research Triangle Institute
Hampton, Virginia

Fred H. Proctor†
Flight Dynamics and Control Division
NASA Langley Research Center
Hampton, Virginia

Abstract

A three-dimensional large eddy simulation model is used to investigate the sensitivity of ambient stratification with turbulence on the behavior of aircraft wake vortices. Modeled ambient turbulence levels range from very weak to moderate, and stratification levels range from strongly stable to unstable. The results of profound significance from this study are: 1) very little sensitivity between vortex linking time and the level of stratification, 2) the mean vortex separation remained nearly constant regardless of stratification and turbulence (at least prior to linking), 3) the wake vortices did not rise regardless of the level of stratification, and 4) for very strong stratification, the vortex stopped descending and quickly dissipated even before vortex linking could occur. These results are supported by experimental data and are contrary to conclusions from other numerical studies that assume laminar flow and/or relatively-low Reynolds numbers.

* Aeronautical Engineer
† Research Scientist, Airborne Systems Competency, AIAA member

Nomenclature

b_o	initial vortex separation
g	acceleration due to gravity
N	Brunt-Vaisala frequency - $[(g/\theta)\,\partial\theta/\partial z]^{0.5}$
N^*	$2\pi N\,(b_o)^2/\Gamma_o$
R_c	vortex core radius
R^*	vortex radius divided by b_o
t	time coordinate
T^*	nondimensional time - $t\,V_o / b_o$
V_o	initial vortex descent velocity-$\Gamma_o/(2\,\pi\,bo)$
x	horizontal coordinate along flight path
y	horizontal coordinate lateral to flight path
z	vertical coordinate
Γ	vortex circulation
Γ_o	initial circulation
ϵ	turbulence (eddy) dissipation rate
ν	kinematic viscosity
ε^*	$(\epsilon\,b_o)^{1/3}\,V_o^{-1}$
θ	potential temperature

I. Introduction

The increase of air traffic volume is placing a greater burden on the existing airport facilities. This has brought about the need to improve the efficiency of the existing airports, air traffic control, and aircraft technology. The National Aeronautics and Space Administration (NASA) is involved in improving air traffic volume by investigating technologies that will

increase traffic volume. This is being done through the Terminal Area Productivity (TAP) program, which contains the Reduced Spacing Operations (RSO) sub-element. Within RSO, being directed by NASA's Langley Research Center, there is being developed an Aircraft VOrtex Spacing System (AVOSS)[1,2,3]. The purpose of AVOSS is to investigate how technology may be used to improve airport capacity by increasing the aircraft arrival rate, while insuring that trailing vortices from a leading aircraft do not endanger following aircraft. The current spacing of aircraft is based on general relationship of how long wake vortices from one aircraft may pose a threat to a following aircraft. The AVOSS is designed specifically to be a demonstration system and includes a wake vortex prediction model that uses current weather-state information. The system also includes real-time feedback from sensors to validate the accuracy of the system predictions. Successful demonstration of the system requires that aircraft spacing be safely reduced from what is now currently acceptable during instrument flight rules.

The success of AVOSS will require the prediction model to be able to integrate the effects of many different atmospheric variables such as turbulence intensity, crosswind, and stratification upon vortex motion and decay. The prediction model of AVOSS is called the AVOSS Predictor Algorithm (APA)[4,5,6] which is being tested and extensively verified with observational data collected during recent field deployments[7,8]. Validated numerical models also can be used to test how the APA behaves in extreme conditions, or can be used to provide guidance for additional development and accuracy. An advantage of numerical models is that they allow the sensitivity of specific atmospheric variables or groups of variables to be studied in a controlled fashion. The two atmospheric variables to be addressed in this paper are stratification (via vertical change in temperature), and ambient turbulence intensity.

The atmosphere which wake vortices are embedded is rarely laminar, even under the presence of strong stratification. The combination of turbulence, stratification, and vortex systems with Reynolds numbers (Γ_o/ν) of the order of 10^7, is necessary to adequately model vortex dynamics that are representative of the real world. Previous numerical studies[9,10,11,12] have been conducted at low-Reynolds number and have not combined all of the three aforementioned parameters in their models. Consequently, their findings have not always been in agreement with experimental[13] and field data[14]

Disagreements have been held for some time regarding the influence of stratification on vortex separation and descent.[15] Realistic numerical simulations are needed in order to address the controversies regarding stratification effects on wake vortex transport. As outlined by Spalart[16], four positions are currently held regarding the effect of stable stratification on vortex descent:

1. the wake vortices descend then rise, oscillating at roughly the Brunt Visalia frequency;
2. the descent rate decreases and stops with the decay of the vortices;
3. the descent continues at an increasing rate; or
4. the descent rate slows then increases.

Controversies also exist regarding whether the vortex separation changes or remains nearly constant when influenced by stratification.

In order to investigate the influence of stratification within realistic atmospheric environments, the present study utilizes a three-dimensional, large-eddy simulation (LES) model called the Terminal Area Simulation System (TASS)[17]. The TASS model is a suitable tool to combine stratification, turbulence and high Reynolds number flow. Furthermore, in previous wake vortex investigations, TASS has demonstrated good agreement with observational data[17,18,19, 20,21].

In this study, TASS simulations are conducted for five intensities of stratification in conjunction with three levels of ambient turbulence intensity. The stratification ranges from strongly stable to unstable. The turbulence levels range from moderate to very weak (relative to typical atmospheric boundary layer turbulence). The results are compared with experimental data. Also examined is the sensitivity of linking time, or time required for a vortex pair to connect, as a function of atmospheric stratification and turbulence intensity. In addition, some of the controversies regarding wake vortices within stratified environments are addressed.

Model Description

The Terminal Area Simulation System (TASS) is a time-split compressible, LES, numerical model formulated within a meteorological framework[17]. The TASS model is currently being used in NASA's wake vortex program to model and understand how aircraft trailing vortices interact with the atmosphere. The model can be used in either two or three-dimensions and consists of prognostic equations: for momentum, potential temperature, pressure deviation, and a massless tracer. [Formulations for water substances are

included in TASS, but omitted in the following description since they are not used in this study.]

The TASS equation set in standard tensor notation is as follows:

Momentum:

$$\frac{\partial u_i}{\partial t} + \frac{H}{\rho_o}\frac{\partial p}{\partial x_i} = -\frac{\partial u_i\, u_j}{\partial x_j} + u_i\,\frac{\partial u_j}{\partial x_j} + g\,(H-1)\delta_{i3} + \frac{1}{\rho_o}\frac{\partial \tau_{ij}}{\partial x_j}$$

Buoyancy Term:

$$H = \left[\frac{\theta}{\theta_o} - \frac{p\,C_v}{P_o C_p}\right]$$

Pressure Deviation:

$$\frac{\partial p}{\partial t} + \frac{C_p\,P}{C_V}\frac{\partial u_j}{\partial x_j} = \rho_o\, g\, u_j\, \delta_{j3}$$

Thermodynamic Equation (Potential Temperature):

$$\frac{\partial \theta}{\partial t} = -\frac{1}{\rho_o}\frac{\partial \theta\,\rho_o u_j}{\partial x_j} + \frac{\theta}{\rho_o}\frac{\partial \rho_o u_j}{\partial x_j} + \frac{1}{\rho_o}\frac{\partial S_j}{\partial x_j}$$

with the *Potential Temperature* being defined as:

$$\theta = T\left(\frac{P_{oo}}{P}\right)^{\frac{R_d}{C_p}}$$

where θ is conserved for dry adiabatic processes.

In the above equations, u_i is the tensor component of velocity, t is time, p is deviation from atmospheric pressure P, T is atmospheric temperature, ρ is the air density, C_p and C_v are the specific heats of air at constant pressure and volume, g is the earth's gravitational acceleration, R_d is the gas constant for dry air, P_{oo} is a constant equivalent to 1000 millibars (10^5 pascals) of pressure. Environmental state variables are defined from the initial input sounding and are functions of height only.

The subgrid flux terms, τ_{ij} for momentum and S_j for potential temperature, are approximated with first order closure. The subgrid eddy viscosity is determined from a modified Smagorinsky model[22] given by the following relationship for the subgrid eddy viscosity:

$$K_M = (c_s\Delta)^2 |D| \left(1 - \alpha_1 Ri_S - \alpha_2 Ri_R\right)$$

where K_M is the subgrid eddy viscosity, Δ is the filter width, D is the rate of deformation, and Ri_S and Ri_R are the Richardson numbers due to stratification and rotation, respectively. The remaining terms, c_s=0.16, α_1=3.0, and α_2=1.5 are constants. The filter width is based on the minimal resolvable scale:

$$\Delta = [\ 2\Delta x\ 2\Delta y\ 2\Delta z\ ]^{1/3}$$

where Δx, Δy, and Δz are the numerical grid sizes in the respective x, y, z direction.

The simulations assume fully-periodic boundary conditions, and thus represent the free atmosphere with no ground effect.

II. Initial Conditions and Model Parameters

A wake vortex simulation is initialized by combining stratification, a well-developed ambient turbulence field, and the initial wake vortex field.

In order to isolate stratification and turbulence effects, the vortex environment assumes neither environmental winds nor any ground effects. Therefore, the wake vortices are affected only from the influence of the stratified environment and ambient turbulence.

Vortex Parameters

The initial vortex system used in this study is representative of the pair of counter-rotating trailing vortices which are formed downstream of a generating aircraft. The initial vortex velocity field for this system is from Proctor[17], and does not include any initial axial velocity. The vortex parameters assumed in all of the experiments are given in table 1.

Table 1. *Initial vortex parameters used for all numerical experiments.*

Parameter	Value	
Vortex spacing (b_0)	36 m	
Vortex core radius (R_c)	4.5 m	(b_0/8)
Vortex circulation (Γ_o)	360 m^2/s	

Stratification parameters

The five different stratification levels chosen for this study are given in table 2. The first level, N^*=1.0, represents a very stable stratification. The last level corresponds to an unstable stratification hence the complex imaginary value for N.

Table 2. *Ambient stratification levels used for the numerical study.*

N^*	N (s^{-1})	$\frac{\partial\theta}{\partial z}$ (°C/km)
1.0	4.42 x 10^{-2}	54.2
0.5	2.21 x 10^{-2}	13.6
0.375	1.66 x 10^{-2}	7.62
0.0	0.0	0.0
-.33 $\sqrt{-1}$	1.46 x 10^{-2} $\sqrt{-1}$	-5.90

Turbulence Initialization

First, a baseline ambient turbulence field is created in the absence of stratification. As in Han *et al.*,[20,23] the resolved-scale turbulence is generated by a two-step process. First, the domain velocities are initialized by a random number generator such that continuity is enforced. Then, energy is added uniformly at wavenumbers less than 3 via a forcing function. The simulation is carried out until the magnitude of the total kinetic energy (TKE) of the domain reaches a quasi-steady state. Figure 1 shows turbulence spectra prior to injecting the wake vortices. The wave number has been scaled such that κ=1 is the initial vortex spacing (b_o). The turbulence is nearly isotropic and contains a well-defined inertial subrange. The spectra in this figure are from the case with the strongest turbulence intensity level, and correspond to a moderate turbulence intensity level in the lower atmosphere[24].

The three values of turbulence intensity chosen for this study are given in table 3. The appendix gives the details of how the TKE of the baseline turbulence field is then scaled to create the other two desired turbulence levels. These turbulence intensities represent typical levels experienced during the early morning hours in the lower atmosphere with the very weak level corresponding to calm conditions[24].

Table 3. *Ambient turbulence intensity levels used for the numerical study. The bold value represents the unscaled turbulence intensity.*

Turbulence Intensity	ε (m^2/s^3)	ε^*
Moderate	**1.35 x 10^{-3}**	**0.23**
Weak	4.0 x 10^{-5}	0.07
Very Weak	1.0 x 10^{-7}	0.01

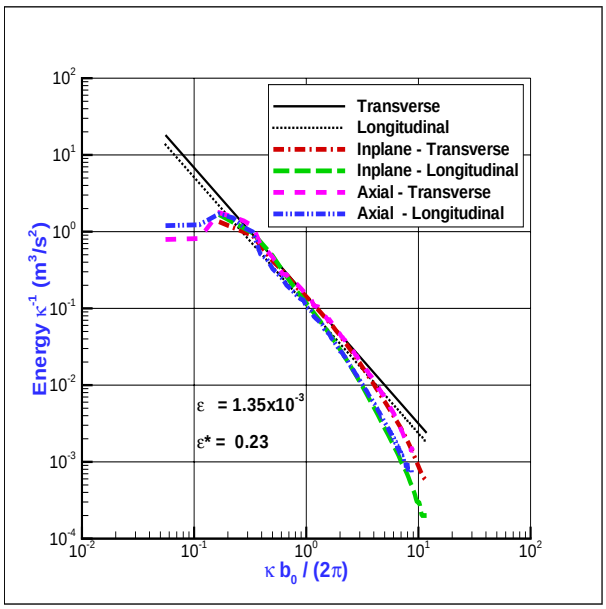

Figure 1. *Turbulent spectra for the TASS model domain prior to vortex insertion. The solid, thin transferse and longitudinal lines represent the theoretical –5/3 slope of the inertial subrange, whereas the dotted and dashed lines represent TASS field spectra.*

Each case simulation is initialized by the following procedure. First, the vortex is initialized within a specific stratification level without any ambient turbulence. Next, the baseline ambient turbulence field is scaled to create the desired turbulence level. Finally, the velocity and pressure fields from the non-turbulent vortex and the ambient turbulence are combined just prior to the start of the simulation.

Model domain parameters

The model domain parameters are shown in table 4. The crossflow width and height are optimally chosen to minimize computing time and reduce interactions with image vortices. The axial domain length is long enough to model the development of the Crow instability for which the maximum theoretical wavelength is 8.6 b_0.[25]

Table 4. *Three-dimensional model domain parameters used for the numerical study.*

Parameter	Value	
Crossplane width/height (L_y, L_z)	216 m	(6 b_0)
Axial length (L_x)	648 m	(18 b_0)
Crossplane resolution (Δy,Δz)	1.5 m	(b_0/24)
Axial resolution (Δx)	2.0 m	(b_0/18)

Numerical experiments performed

Simulations are performed at each stratification level for the moderate and weaker turbulence intensity levels. Table 5 displays the groupings of the ten simulations. Note that the lowest value of turbulence intensity has been chosen only for the strongly stratified case. Together these cases encompass typical levels for both stratification and turbulence experienced in the lower atmospheric boundary layer. All simulations in this study assume a rotational Reynolds number of (Γ_o/ν) of ~ 10^7, as is the case for atmospheric wake vortices.

Table 5. *Matrix of stratification and turbulence intensity levels used for the numerical study.*

Stratification Level	Moderate Turbulence	Weak Turbulence
N* = 1.0	0.23	0.01
N* = 0.5	0.23	0.07
N* = 0.375	0.23	0.07
N* = 0.0	0.23	0.07
N* = -0.33	0.23	0.07

Runtime parameters

Circulation is computed for each vortex where the vorticity vector is within 30° of the crossflow plane vector. The circulation at a given radius is then computed by the following relationship:

$$\Gamma_r = \iint \zeta dA ,$$

where ζ is the axial component of vorticity. The restriction on vortex alignment minimizes any artificial decay of circulation due to skewness with the axial vorticity vector. However, the position of a vortex is still used regardless of the skewness of the vorticity vector with the crossflow plane. The actual circulation value used in this study is an averaged value given by the following relationship:

$$\overline{\Gamma}^{a,b} = \frac{\int_a^b \Gamma_r \, dr}{\int_a^b dr} ,$$

For this paper, the average circulation is taken from *a=5* to *b=15* meters, which is a suitable metric for representation of the vortex hazard[26].

In addition to the circulation, four other parameters are monitored during the course of each run. They are height, lateral separation, descent velocity, and linking factor. The first three parameters are domain average quantities for each vortex of the system. The domain average is computed from the mean values of all crossflow planes where a vortex is found. The criterion for a valid vortex is when the tangential velocity exceeds *4.85 m/s*. The final parameter or growth parameter, the linking factor, is defined as:[25]

$$\beta(t) = \frac{b_{max} - b_{min}}{b_{max} + b_{min}} ,$$

where b_{max} and b_{min} are the maximum and minimum lateral vortex separation in a given plane, respectively. The vortex system is considered linked when the linking factor is 0.85 or greater and coherent ring-like structures are present.

III. Results

The model results are first compared with experimental data for the vortex time to link and height profiles. Next, after establishing the accuracy of the model, three-dimensional perspectives of the vortex system are examined for the weaker turbulence levels. Finally, the domain mean quantities for position and circulation are presented.

Experimental Comparisons

As in a previous study with the TASS model for neutral stratification, the vortex linking time was found to be a function of nondimensional eddy dissipation[23]. The present study includes the influence of stratification on vortex linking time. The results showed very little influence from stratification. However, the cases with *N**=1.0 did not link before the vortex dissipated. This agrees with previous experimental data showing linking did not occur when *N** is greater than *0.75*[13]. The time variation of the growth parameter for the cases that linked is shown in fig. 2. Each of the turbulence levels shows an exponential growth rate that is independent of the level of stratification. Furthermore, the increase of turbulence reduces the vortex time to link. The exponential growth rates in fig. 2 are similar to those presented in fig. 10 of Sarpkaya[13].

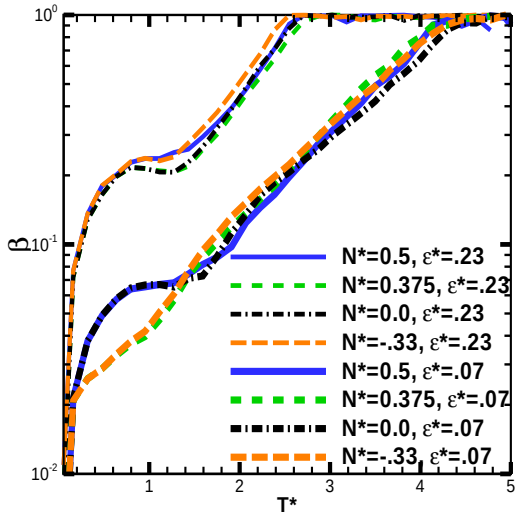

Figure 2. *Time variation of vortex linking factor for cases where linking occurred.*

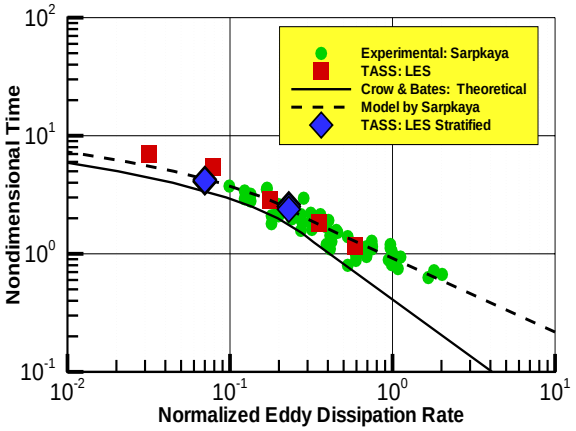

Figure 3. *Vortex time to link as a function of eddy dissipation rate. The results from the current study are represented by the diamonds.*

Figure 3 shows a comparison of the time to link with experimental data[27], and theory[28,29], and previous TASS results[23]. The present TASS results closely match the theoretical predictions of Sarpkaya irrespective of stratification.

The comparison of vortex descent with experimental results of Sarpkaya[13] is shown in fig. 4-6. In each of these figures are results from TASS assuming turbulent and laminar flow. The presence of turbulence, albeit very weak, inhibits any acceleration in the descent as is apparent in the laminar simulation. For strong stable stratification with turbulence, the vortex descent stops and the vortices rapidly decay. Although the laminar simulations show a rapid acceleration after a stall, this is not likely to occur because the atmosphere is rarely laminar. For the *N*=1.0* case, the presence of turbulence rather than its magnitude appears to be significant, since the results from the weak and moderate turbulence intensity are essentially the same. Not in any of the cases did the stable stratification cause the vortices to rise. These experiments demonstrate that *high Reynolds number flow with turbulence is required to correctly model atmospheric wake vortices in stratified environments.*

Figures 4-6 display excellent agreement with the laboratory results. Specifically for *N**=1.0, the results show little dependency upon the intensity of turbulence.

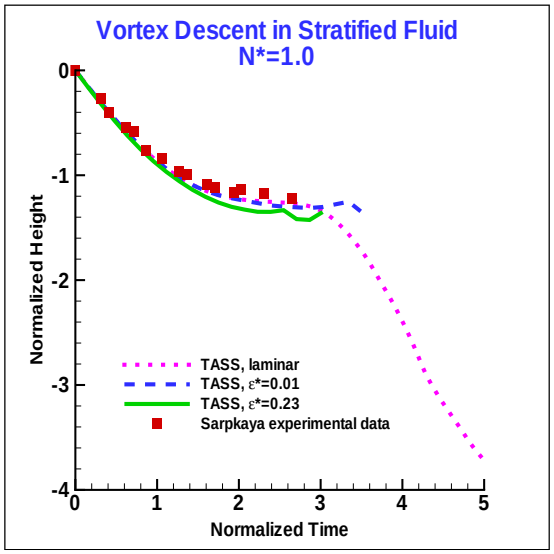

Figure 4. *Comparison of TASS model results from turbulent and laminar simulations with experimental data from Sarpkays[13] at strong stratification (N*=1.0). The dotted, dashed and solid lines represent laminar, weak turbulence, and moderate turbulence results, respectively.*

TASS Model Results Analysis

The orthographic projection of the three-dimensional vortex domain is shown in fig. 7-9. In each figure, the vortex is identified by the second eigenvalue, λ_2, of the symmetric tensor $S^2 + \Omega^2$, where S and Ω are the symmetric and antisymmetric components of the stress tensor ∇u, respectively[30]. Han[23] et al. applied this method of vortex identification

and showed the isosurface of negative values of λ_2 to capture the structure of the vortex system very well.

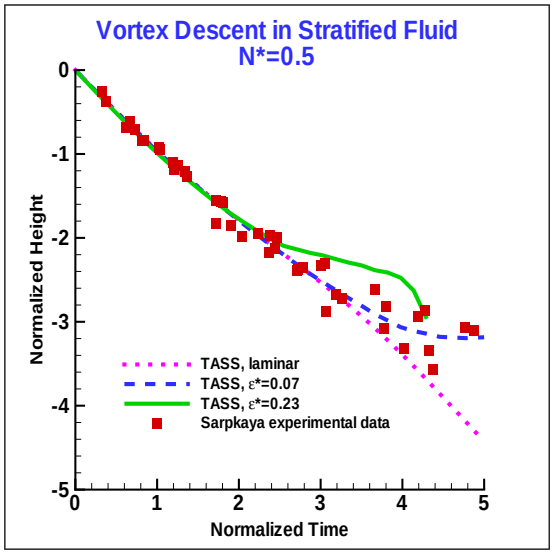

Figure 5. *Same as figure 4, but for stratification of N*=0.5.*

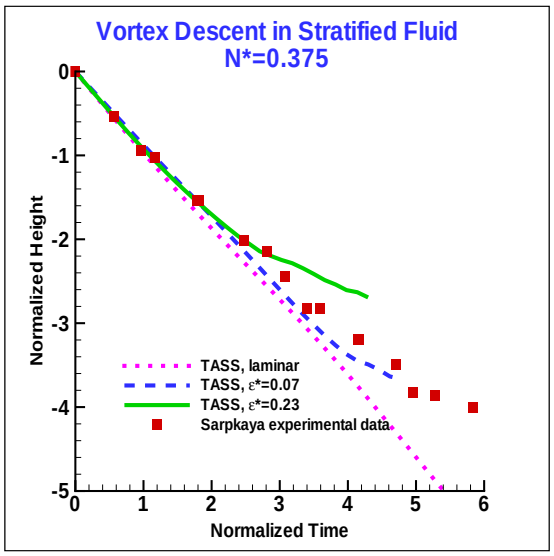

Figure 6. *Same as figure 4, but for N*=0.375 stratification.*

The time evolution for neutral stratification (*N*=0*) shows the larger wavelength instability due to Crow but no small-scale instabilities (fig. 7). The vortex system descends uniformly until vortex linking occurs around *T** of 4.3. After which time, the regions of reduced lateral separation accelerate downward creating a bending of the isosurface in the side view. After the linking time, the vortex system degenerates into a series of rings that quickly dissipates (not shown).

In fig. 8, the results at the same turbulence intensity for *N*=0.5* are shown. Similar trends are reproduced, namely the uniform descent, the bending of the isosurface, and the time of vortex linking. The important difference is the onset of small-scale instabilities around *T*=2.5*. Rapid dissipation occurs at *T** of *4.3*, where the vortex lateral separation is a local maximum.

The strongly stratified case with very weak turbulence is shown in fig. 9. The two striking observations for this case are: 1) the wavelengths of the sinusoidal instabilities are much smaller than *8.6* b_0, and 2) the vortex dissipates well before the theoretical time to link of *7.3 T**. The shorter wavelengths prevent vortex linking while also seeming to accelerate the rate of decay of the system. The vortex never develops an instability with wavelengths greater than b_0 prior to dissipating. The *N*=0.5* case in fig. 8 showed both the long and short wavelength instabilities. This suggests a critical level of stratification somewhere between 0.5 and 1.0 where the short waves dominate.

The dynamics of the vortex evolution can be viewed in another format. The evolution of the radial profile of mean circulation and tangential velocity are shown in fig. 10. The plots in this figure are for the same cases as in figs. 7-9. The neutral stratification (*N**=0.0) shows the strength of the vortex to be maintained up to the linking time. The decrease of circulation for the *N*=0.5* case is more rapid and mostly uniform with radius. For the *N*=1.0* case, two different decay mechanisms are evident. Early on, the circulation decays at the outer edge (*R*>0.6*) while the inner region remains nearly unchanged up until *T**=2.0. The decay at the outer edge most likely results from opposite sign vorticity generated by the stratification while the inner region decay is due to turbulence. The tangential velocity shows that the core radius remains constant up to vortex dissipation. This figure demonstrates that the circulation near the core remains strong until the time of vortex dissipation.

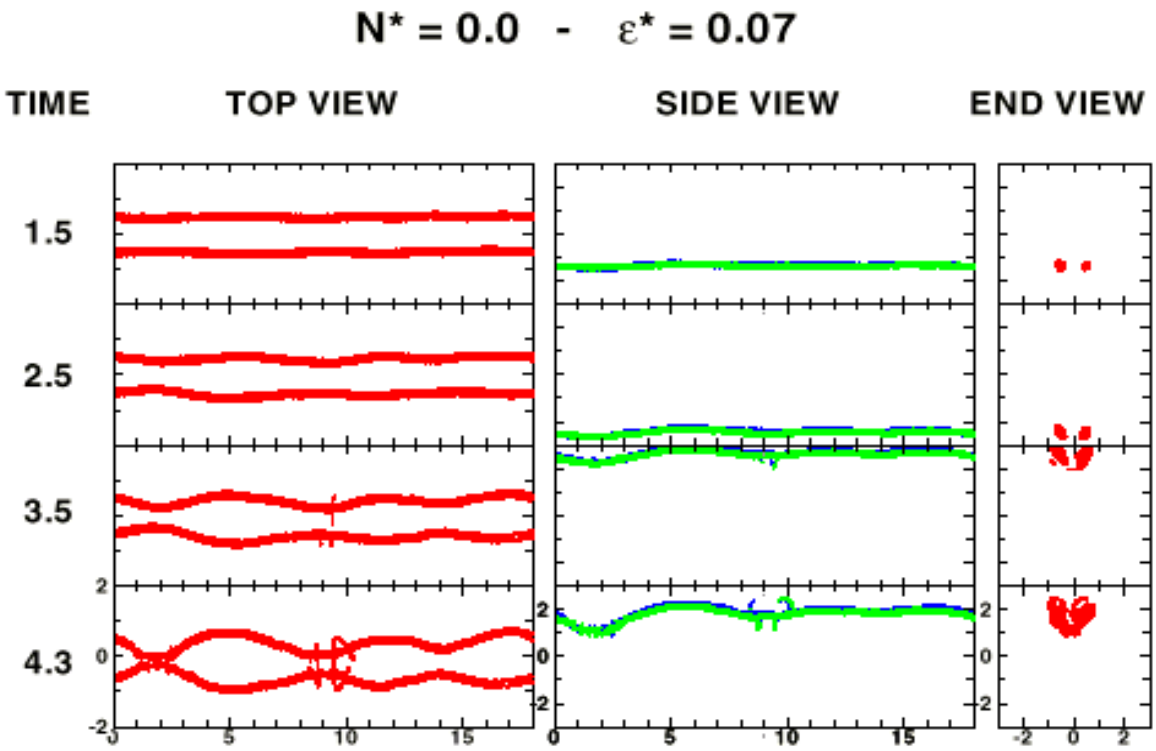

Figure 7. *Time evolutions of orthographic projections of the vortex structure of TASS model results for the case N*=0 and ε*=0.07. The projections are shown at four nondimensional times. The last time corresponds to the theoretical time to link. The time for each top, side, and end view is labeled to the left of each row. The domain dimensions are shown at the bottom row and are given in b_o units.*

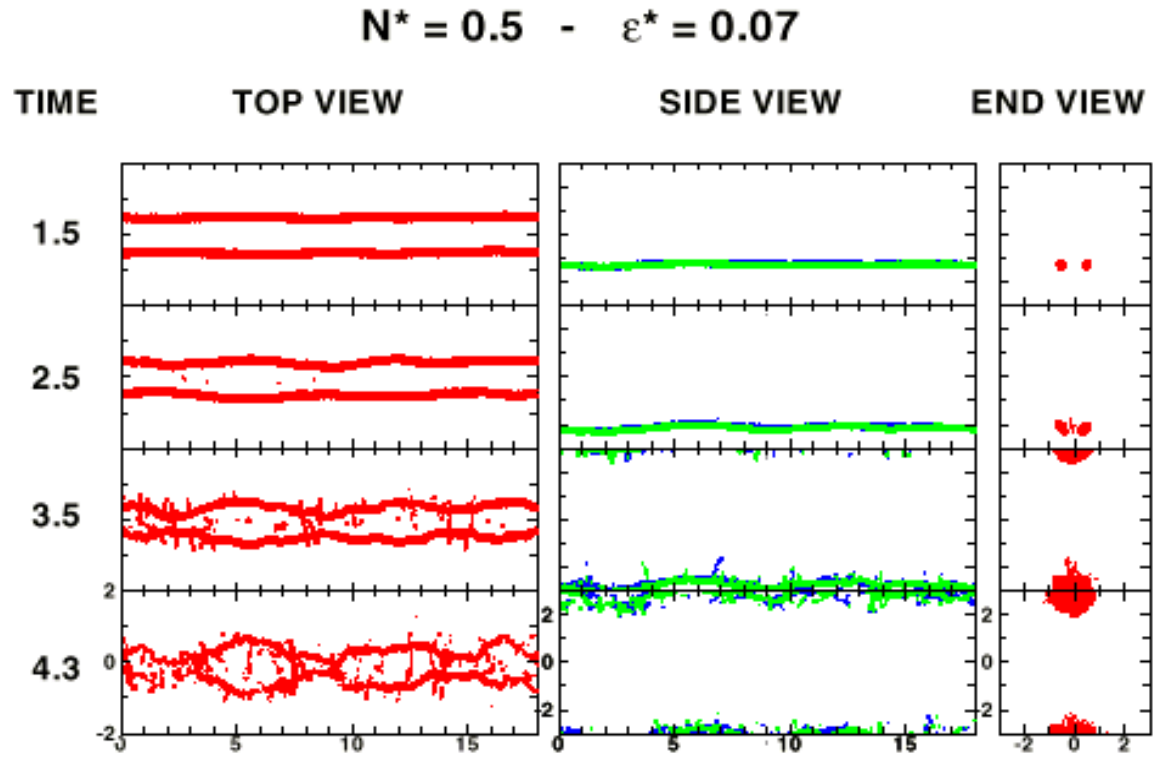

Figure 8. *Same as figure 7, but for N*=0.5.*

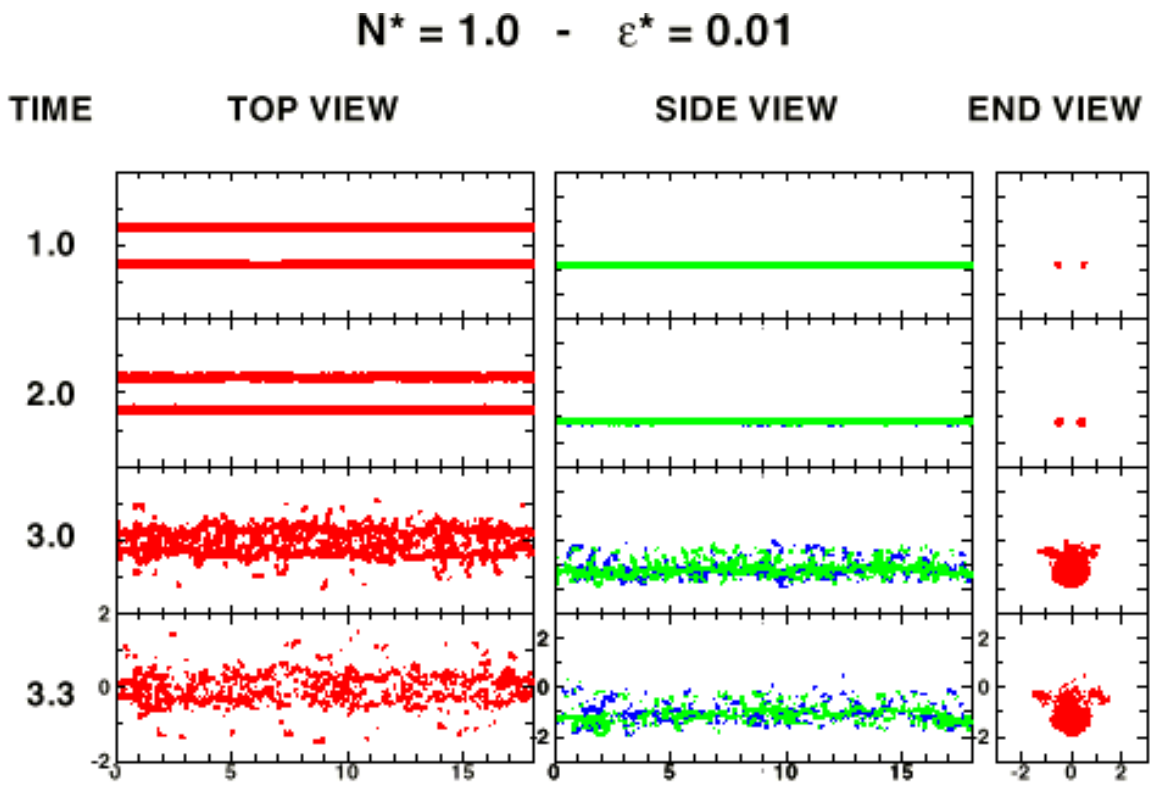

Figure 9. *Same as figure 7, but for N*=1.0 and ε*=0.01. The last time is shortly before the vortex dissipates.*

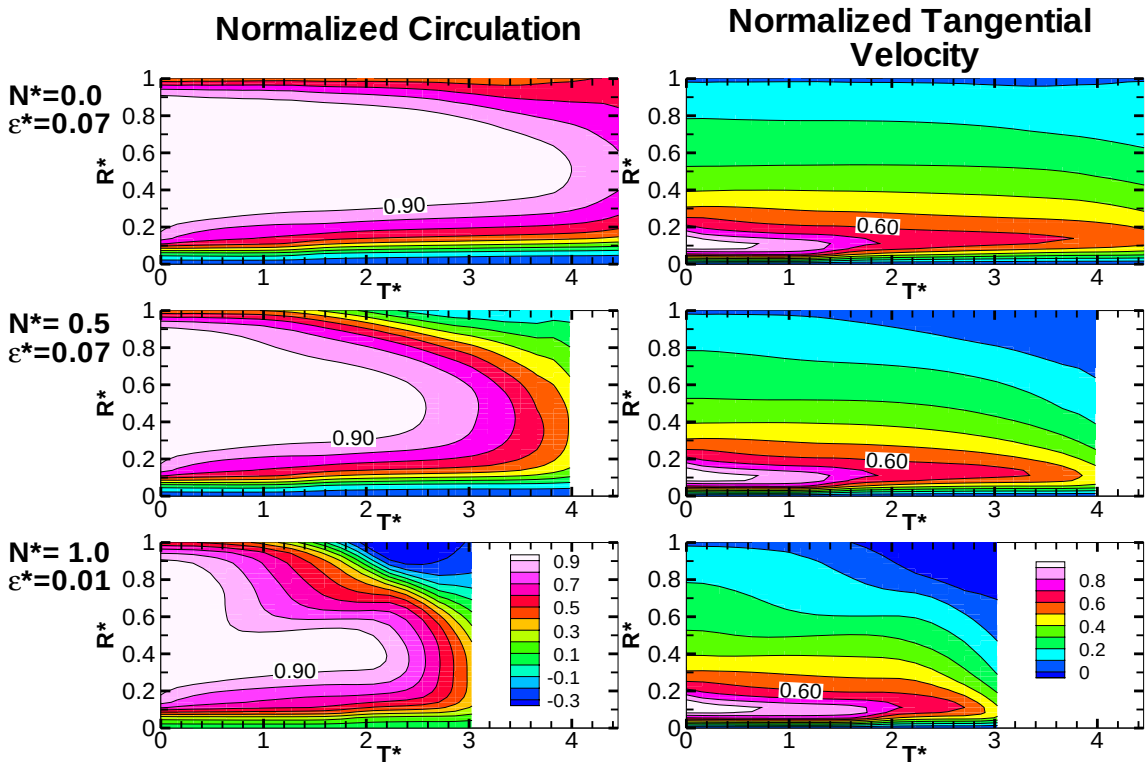

Figure 10. *Time evolution of axially averaged radial profile of circulation and tangential velocity for N* of 0.0, 0.5 and 1.0 at the weak turbulence intensity levels. Radial (R*) distance is normalized by b_0. Circulation and tangential velocity are normalized by the peak value at T*=0.*

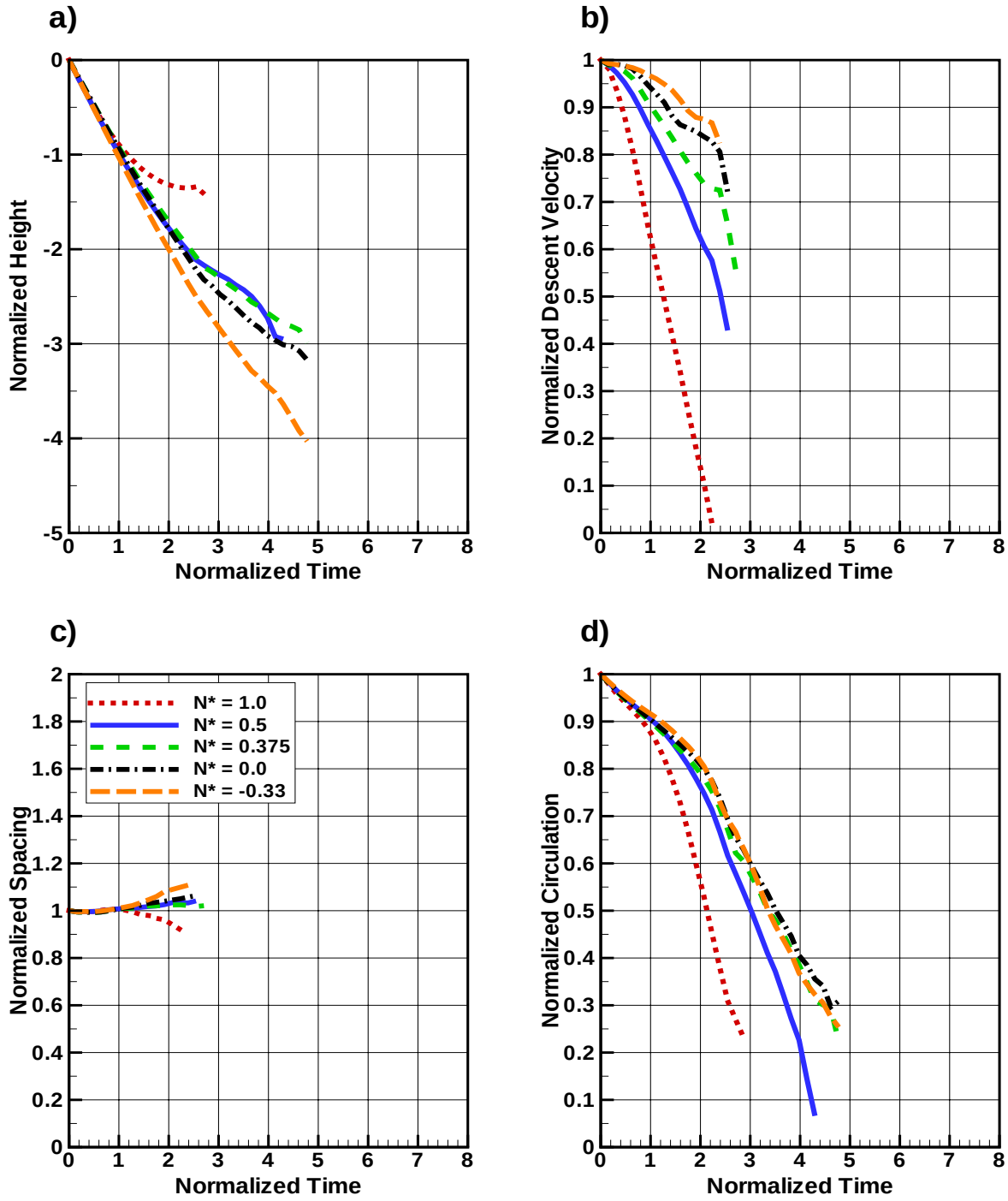

Figure 11. *TASS model results for moderate turbulent intensity level (ε*=0.23). The figures are as follows: a) is the normalized vortex height, b) is the normalized descent velocity (positive downward), c) is the normalized separation, and d) is the vortex circulation. The dotted, solid, dashed, dash-dot and long dashed lines correspond to stratification levels of 1.0, 0.5, 0.375, 0.0, and –0.33, respectively. The legend in c) applies to all plots.*

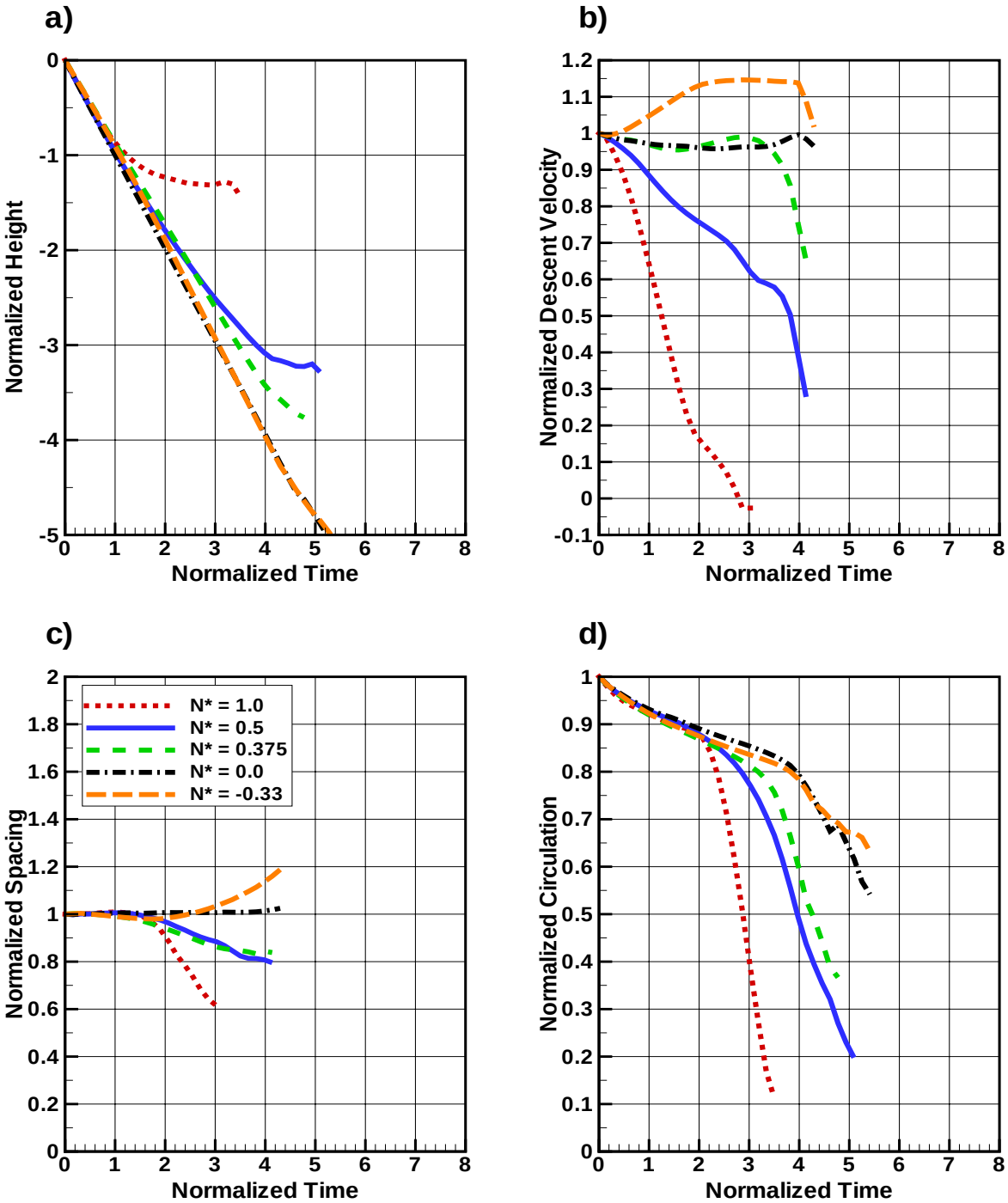

Figure 12. *Same as figure 11, but for weaker turbulent intensity levels (ε*=0.07 or 0.01). The very weak turbulent intensity level is only for the N*=1 case.*

The vortex mean quantities for all moderate turbulence level cases are shown in fig. 11 and for weak turbulence cases in fig. 12. Figures 11a and 11b show that the unstable stratification maintains the greatest descent rate, while in contrast, the N^*=1.0 results show the descent velocity to quickly diminish with the vortex dissipating thereafter. The vortex spacing for all moderate turbulence cases (fig. 11c) remain nearly constant. The circulation for all moderate turbulence cases (fig. 11d) shows stratification begins to become significant for values of N^* greater than 0.5.

For the weaker turbulence intensities, the descent of the vortex system is sustained longer (fig. 12b). For the unstable stratification, (N^*=-0.33) the generation of same sign vorticity increases the vortex descent rate. This rate of descent remains greater than the vortex initial value until near the end of the vortex lifetime. The vortex separation remains nearly constant (fig. 12c) except for increasing slightly for unstable stratification and increasing slightly for stable stratification. The changes in vortex separation for the weak turbulence case are slightly greater than the changes for the moderate turbulence cases (cf., fig 11c).

IV. Summary and Conclusions

This study of aircraft wake vortices within turbulent, thermally stratified domains without surface effects has been performed using a validated three-dimensional LES model. The case simulations encompassed turbulence and stratification levels typical of the lower atmosphere. The results show that turbulence and high Reynolds numbers are required to properly model the evolution of vortices in stratified fluids.

The primary conclusions of this study are:

1. Strong stable stratification may suppress vortex linking; otherwise, stratification alone has negligible effect upon vortex linking time.

2. The critical stratification level above which vortices no longer link is between 0.5 and 1.0.

3. In strong stratification, a vortex may contain hazardous circulation levels near the core until just prior to dissipating.

4. The mean vortex separation remains nearly constant until either the vortex decays or linking occurs.

5. Aircraft wake vortices were not found to rise within realistic atmospheric environments containing strong stable stratification. Instead, the descent was arrested by the stratification, and the vortices decayed rapidly after stalling.

6. The presence of the slightest amount of turbulence is necessary to properly model vortex dynamics in stratified domains.

Acknowledgements

This research was sponsored by NASA's Terminal Area Productivity Program. One of the authors was funded under contract NAS1-99074. Numerical simulations were carried out at NASA's Aeronautics Consolidated Supercomputing Facility.

Appendix -- Turbulence Scaling

The turbulence intensity level is related to the TKE by the following relationship:

$$(\mathrm{TKE})^{3/2} = C\,\varepsilon\,,$$

where C is a proportionality constant. Therefore, the scaling of the TKE will also scale the eddy dissipation rate. Introducing a scaling constant into the above equation gives:

$$\left(\frac{\mathrm{TKE}}{\alpha}\right)^{3/2} = (\mathrm{TKE}_{new})^{3/2} \cong C\,\varepsilon_{new}\,,$$

where α is the scaling constant. The scaling of the TKE is achieved by scaling the velocity components. The definition of TKE is needed to determine how the scaling constant is to be applied to the velocity components. TKE is defined as:

$$\mathrm{TKE} \equiv \frac{1}{2}\sum\left(U^2 + V^2 + W^2\right),$$

where U, V, and W are the velocity components. Introducing the scaling parameter into the above gives:

$$\mathrm{TKE}_{new} \equiv \frac{1}{2}\sum\left(\left(\frac{U}{\sqrt{\alpha}}\right)^2 + \left(\frac{V}{\sqrt{\alpha}}\right)^2 + \left(\frac{W}{\sqrt{\alpha}}\right)^2\right).$$

Define the scaled velocities as:

$$U^* \equiv \frac{U}{\sqrt{\alpha}},\ V^* \equiv \frac{V}{\sqrt{\alpha}},\ \text{and}\ W^* \equiv \frac{W}{\sqrt{\alpha}},$$

then the new TKE becomes:

$$\mathrm{TKE}_{\mathrm{new}} \equiv \frac{1}{2}\sum\left(\left(U^*\right)^2 + \left(V^*\right)^2 + \left(W^*\right)^2\right).$$

The first test is to determine if the scaling parameter affects mass continuity. For incompressible flow:

$$\frac{\partial U}{\partial x} + \frac{\partial V}{\partial y} + \frac{\partial W}{\partial z} = 0 .$$

Substituting the relationship for the scaled velocity components into the mass continuity equations gives:

$$\sqrt{\alpha}\left(\frac{\partial U^*}{\partial x} + \frac{\partial V^*}{\partial y} + \frac{\partial W^*}{\partial z}\right) = 0 .$$

Therefore, mass continuity is maintained by the scaling of the velocity components.

The next test is to determine how scaling affects the momentum equations. The momentum equation in the x direction for an incompressible, adiabatic, and neutrally stratified fluid can be written as:

$$\frac{\partial U}{\partial t} + U\frac{\partial U}{\partial x} + V\frac{\partial U}{\partial y} + W\frac{\partial U}{\partial z} + \frac{1}{\rho}\frac{\partial P}{\partial x} = 0 ,$$

where t represents time and P pressure. Substituting the scaled velocity components into this momentum equation results in the following:

$$\sqrt{\alpha}\frac{\partial U^*}{\partial t} + \alpha\left[U^*\frac{\partial U^*}{\partial x} + V^*\frac{\partial U^*}{\partial y} + W^*\frac{\partial U^*}{\partial z}\right] + \frac{1}{\rho}\frac{\partial P}{\partial x} = 0$$

Introducing the following relationships for time and pressure:

$$t^* \equiv t\sqrt{\alpha} \text{ , and } P^* \equiv \frac{P}{\alpha},$$

results in the following for the momentum equation:

$$\alpha\left[\frac{\partial U^*}{\partial t^*} + U^*\frac{\partial U^*}{\partial x} + V^*\frac{\partial U^*}{\partial y} + W^*\frac{\partial U^*}{\partial z} + \frac{1}{\rho}\frac{\partial P^*}{\partial x}\right] = 0 .$$

The same scaling is also applied to the momentum equations in the y and z directions.

Therefore, the procedure to scale the TKE involves scaling of the velocity components and the pressure to maintain mass continuity without disturbing the balance between pressure and momentum.

References

[1]Hinton, D. A., Charnock, J. K., Bagwell, D. R., and Grigsby, D., "NASA Aircraft Vortex Spacing System Development Status," *37th Aerospace Sciences Meeting & Exhibit*, Reno, NV, AIAA-99-0753, January 1999, 17 pp.

[2]Hinton, D. A., "Aircraft Vortex Spacing System (AVOSS) Conceptual Design," NASA Tech Memo No. 110184, August 1995, 27 pp.

[3]Perry, R. B., Hinton, D. A., and Stuever, R. A., "NASA Wake Vortex Research for Aircraft Spacing," *35th Aerospace Sciences Meeting & Exhibit*, Reno, NV, AIAA Paper No. 97-0057, January 1997, 9 pp.

[4]Sarpkaya, T., "A New Model for Vortex Decay in the Atmosphere," *37th Aerospace Sciences Meeting & Exhibit*, Reno, NV, AIAA-99-0761, January 1999, 14 pp.

[5]Robins, R.E., Delisi, D.P. and Greene, G.C., "Development and Validation of a Wake Vortex Prediction Algorithm," 36th Aerospace Sciences Meeting & Exhibit, AIAA-98-0665, January 1998, 10 pp.

[6]Sarpkaya, T., Robins, R.E., and Delisi, D.P., "Wake-Vortex Eddy-Dissipation Model Predictions Compared with Observations," 38th Aerospace Sciences Meeting & Exhibit, AIAA-2000-0625, January 2000.

[7]Heinrichs, R. M., Dasey, T. J., Matthews, M. P., Campbell, S. D., Freehart, R. E., Perras, G. H. and Salamitou, P., "Measurements of Aircraft Wake Vortices at Memphis International Airport with a CW CO_2 Coherent Laser Radar," SPIE Symposium on Aerospace/Defense Sensing and Controls, Air Traffic Control Technologies II, SPIE-2737-20, Orlando, FL, April 1996, 11 pp.

[8]Britt, C. L., Nguyen, D. P. C., and Koch, G., "Pulsed Lidar Measurements of Aircraft Wake Vortices at DFW and JFK," *37th Aerospace Sciences Meeting & Exhibit*, AIAA-99-0982, Reno, NV, January 1999, 10 pp.

[9]Spalart, P. R., "Airplane Trailing Vortices," *Ann. Rev. Fluid Mech.*, Vol. 30, 1998.

[10]Garten, J. F., Arendt, S., Fritts, D. C., and Werne, J., "Dynamics of Counter-Rotating Vortex Pairs in Stratified and Sheared Environments," *J. Fluid Mech.*, Vol. 361, 1998, pp. 189-236.

[11]Holzapfel F., and Gerz, T., "Two-dimensional Wake Vortex Simulations in the Stably Stratified Atmosphere," *2nd Fluid Dynamics Conf.*, AIAA-98-2857, Albuquerque, NM, June 1998, 9 pp.

[12]Robins, R. E., and Delisi, D. P., "Numerical Simulation of Three-Dimensional Trailing Vortex Evolution in Stratified Fluid," *AIAA Journal*, Vol. 36, No. 6, 1998, pp. 981-985.

[13]Sarpkaya, T., "Trailing Vortices in Homogeneous and Density-stratified Media," *Journal of Fluid Mech.*, Vol. 136, 1983, pp. 85-109.

[14] Tombach, I., "Observations of Atmospheric Effects on Vortex Wake Behavior," *J. Aircraft*, Vol.10, No. 11, 1973, pp. 641-647.

[15]Widnall, S., 1975, "The Structure and Dynamics of Vortex Filaments," *Annual Review of Fluid Mechanics*, Vol. 7, 1975, pp. 141-165.

[16]Spalart, P., 1997, "Wake Vortex Physics: The Great Controversies," Proceedings of the NASA First Wake Vortex Dynamic Spacing Workshop, NASA CP-97-206235, November 1997, pp. 33-44.

[17]Proctor, F. H., "Numerical simulation of wake vortices measured during the Idaho Falls and Memphis field programs. *14th AIAA Applied Aerodynamics Conference*, Proceedings, Part- II, 17-20 June 1996, New Orleans, LA, AIAA Paper No. 96-2496, pp. 943-960.

[18]Proctor, F. H., and Han, J., "Numerical Study of Wake Vortex Interaction with the Ground Using the Terminal Area Simulation System," *37th Aerospace Sciences Meeting & Exhibit*, AIAA-99-0754, Reno, NV, January 1999, 12 pp.

[19]Proctor, F.H., "The NASA-Langley Wake Vortex Modelling Effort in Support of an Operational Aircraft Spacing System," 36th Aerospace Sciences Meeting & Exhibit, AIAA-98-0589, January 1998, 19 pp.

[20]Han, J., Lin, Y.-L., Arya, S.P., and Proctor, F.H., "Numerical Study of Wake Vortex Decay and Descent within Homogeneous Turbulence," In press, *AIAA Journal*, Vol. 38, 2000.

[21]Shaohua, S., Ding, F., Han, J., Lin, Y-L., Arya, S. P., and Proctor, F. H., "Numerical Modeling Studies of Wake Vortices: Real Case Simulations," *37th Aerospace Sciences Meeting & Exhibit*, AIAA-99-0755, Reno, NV, January 1999, 16 pp.

[22]Smagorinsky, J., "General Circulation Experiments with the Primitive Equations: 1. The Basic Experiment," *Mon. Wea. Rev.*, Vol. 93, 1963, pp. 727-768.

[23]Han, J., Lin, Y.-L., Schowalter, D. G., Arya, S. P., and Proctor, F. H., "Large Eddy Simulation of Aircraft Wake Vortices within Homogeneous Turbulence: Crow Instability," *AIAA Journal*, Vol. 38, February 2000.

[24]Stull, R.B., *An Introduction to Boundary Layer Meteorology*, Kluwer Academic Publishers, 1988.

[25]Crow, S.C., "Stability Theory for a Pair of Trailing Vortices," *AIAA Journal*, Vol. 8, No. 12, December 1970, pp. 2172-2179.

[26]Hinton, D. A. and Tatnall, C. R., "A Candidate Wake Vortex Strength Definition for Application to the NASA Aircraft Vortex Spacing System (AVOSS)," NASA Tech Memo No. 110343, Sept. 1997, 32 pp.

[27]Sarpkaya, T., and Daly, J. J., "Effect of Ambient Turbulence on Trailing Vortices," *Journal of Aircraft*, Vol., 24, No, 6, 1987, pp. 399-404.

[28]Sarpkaya, T., "Decay of Wake Vortices of Large Aircraft," *AIAA Journal*, Vol 36, 1998, pp. 1671-1679.

[29]Crow, S. C., and Bate, E. R., "Lifespan of Trailing Vortices in a Turbulent Atmosphere," *Journal of Aircraft*, Vol. 13, No. 7, 1976, pp. 476-482.

[30]Jeong, J. and Hussain F., "On the Identification of a Vortex," *Journal of Fluid Mech.*, Vol. 285, pp. 69-94.